while the conservative joint 99% confidence limits allow Ω_m values in the range 0.3–0.9 and Ω_Λ values in the range 0.1–1.4. The constraints obtained separately from Mark III and SFI are very similar.

The constraints from local flows thus remove the degeneracy in the constraints from the global-geometry test based on supernovae (and vice versa), and help rule out an open model with zero cosmological constant. A nearly flat universe, with comparable contributions of matter and cosmological constant to the total energy density, is likely. The favoured model is therefore an unbound universe that will accelerate forever, although it is still impossible yet to determine whether the global geometry is flat, open or closed.

Such comparable contributions from the mass density and the cosmological constant represent a puzzling fine tuning, for example because the two parameters, Ω_m and Ω_Λ, are expected to vary with time in opposite senses. The standard theory expects the cosmological constant either to vanish or be larger by many orders of magnitude[8,23]. Perhaps entropic arguments may be needed to explain such a fine tuning. Although the observed constraints are not yet finally confirmed, they already seem interesting enough to pose a serious challenge to theoretical physics.

Other constraints in the Ω_m–Ω_Λ plane are worth mentioning in this framework. Constraints consistent with the supernova ridge but of larger uncertainty arise from the age of old star clusters[24] versus the Hubble expansion rate. Constraints of orthogonal orientation, roughly on $\Omega_\Lambda + \Omega_m$, can be deduced from the acoustic peaks in the sub-degree angular power spectrum of fluctuations in the CMB, as observed from balloons and from the ground[22,25–29]. Two CMB satellites planned for the next decade, MAP and Planck, are expected to provide more accurate constraints[27,30].

Future peculiar-velocity data are expected to improve the accuracy of the constraints. In addition to many new velocities based on distance indicators of the Tully–Fisher type, the most promising sources of large-scale peculiar velocities in the future will probably be the siblings of the same supernovae discussed above, but at low redshifts; their distances can be measured with 5–10% accuracy out to large distances and their sampling density is limited only by the patience of the observers. □

1. Perlmutter, S. *et al.* Measurements of Ω and Λ from 42 high-redshift supernovae. *Astrophys. J.* **517**, 565–586 (1999).
2. Riess, A. G. *et al.* Observational evidence from supernovae for an accelerating universe and a cosmological constant. *Astron. J.* **116**, 1009–1038 (1998).
3. Dekel, A. & Rees, M. J. Ω from velocities in voids. *Astrophys. J.* **422**, L1–L4 (1994).
4. Nusser, A. & Dekel, A. Ω and the initial fluctuations from velocity and density fields. *Astrophys. J.* **405**, 437–448 (1993).
5. Bernardeau, F., Juszkiewicz, R., Dekel, A. & Bouchet, F. R. Omega from the skewness of the cosmic velocity divergence. *Mon. Not. R. Astron. Soc.* **274**, 20–26 (1995).
6. Zaroubi, S., Zehavi, I., Dekel, A., Hoffman, Y. & Kolatt, T. Large-scale power spectrum from peculiar velocities via likelihood analysis. *Astrophys. J.* **486**, 21–31 (1997).
7. Freudling, W. *et al.* Large-scale power spectrum and cosmological parameters from SFI peculiar velocities. *Astrophys. J.* **532**, (in press); also as preprint astro-ph/9904118 (1999).
8. Carroll, S. M., Press, W. H. & Turner, E. L. The cosmological constant. *Annu. Rev. Astron. Astrophys.* **30**, 499–542 (1992).
9. Willick, J. A. *et al.* Homogeneous velocity–distance data for peculiar velocity analysis. III. The Mark III catalog of galaxy peculiar velocities. *Astrophys. J.* (suppl.) **109**, 333–366 (1997).
10. Haynes, M. P. *et al.* The I-band Tully–Fisher relation for Sc galaxies: optical imaging data. *Astron. J.* **117**, 1668–1687 (1999).
11. Haynes, M. P. *et al.* The I-band Tully–Fisher relation for Sc galaxies: 21 centimeter HI line data. *Astron. J.* **117**, 2039–2051 (1999).
12. Dekel, A. *et al.* POTENT reconstruction from Mark III velocities. *Astrophys. J.* **522**, 1–38 (1999).
13. Dekel, A., Bertschinger, E. & Faber, S. M. Potential, velocity, and density fields from sparse and noisy redshift-distance samples: Method. *Astrophys. J.* **364**, 349–369 (1990).
14. Sugiyama, N. Cosmic background anisotropies in cold dark matter cosmology. *Astrophys. J.* (suppl.) **100**, 281–305 (1995).
15. Sigad, Y., Eldar, A., Dekel, A., Strauss, M. A. & Yahil, A. IRAS versus POTENT density fields on large scales: biasing and omega. *Astrophys. J.* **495**, 516–532 (1998).
16. Eke, V. R., Cole, S., Frenk, C. S. & Henry, P. J. Measuring Ω_0 using cluster evolution. *Mon. Not. R. Astron. Soc.* **298**, 1145–1162 (1998).
17. Dekel, A. & Lahav, O. Stochastic nonlinear galaxy biasing. *Astrophys. J.* **520**, 24–34 (1999).
18. Bunn, E. F. & White, M. The four-year COBE normalization and large-scale structure. *Astrophys. J.* **480**, 6–21 (1997).
19. Lahav, O., Lilje, P. B., Primack, J. R. & Rees, M. J. Dynamical effects of the cosmological constant. *Mon. Not. R. Astron. Soc.* **251**, 128–136 (1991).
20. Riess, A. G., Press, W. H. & Kirshner, R. P. A precise distance indicator: type Ia supernova multicolour light-curve shape. *Astrophys. J.* **473**, 88–109 (1996).
21. Freedman, W. L. in *Critical Dialogues in Cosmology* (ed. Turok, N.) 92–129 (World Scientific, Singapore, 1997).
22. Bond, J. R. & Jaffe, A. H. Constraining large scale structure theories with the cosmic background radiation. *Phil. Trans. R. Soc. Lond. A* (in the press); also as preprint astro-ph/9809043 (1998).
23. Weinberg, S. The cosmological constant problem. *Rev. Mod. Phys.* **61**, 1–23 (1989).
24. Chaboyer, B., Demarque, P., Kernan, P. J. & Krauss, L. M. The age of globular clusters in light of Hipparcos: Resolving the age problem? *Astrophys. J.* **494**, 96–110 (1998).
25. Efstathiou, G., Bridle, S. L., Lasenby, A. N., Hobson, M. P. & Ellis, R. S. Constraints on Ω_Λ and Ω_m from distant type Ia supernovae and cosmic microwave background anisotropies. *Mon. Not. R. Astron. Soc.* **303**, L47–L52 (1999).
26. Lineweaver, C. H. The cosmic microwave background and observational convergence in the Ω_m–Ω_Λ plane. *Astrophys. J.* **505**, L69–L73 (1998).
27. Tegmark, M., Eisenstein, D. J., Hu, W. & Kron, R. Cosmic complementarity: probing the acceleration of the universe. *Astrophys. J.* (submitted); also as preprint astro-ph/9805117 (1998).
28. White, M. Complementary measures of the mass density and cosmological constant. *Astrophys. J.* **506**, 495–501 (1998).
29. Lasenby, A. W., Jones, A. W. & Dabrowski, Y. Observations of the cosmic microwave background and implications for cosmology and large scale structure. *Phil. Trans. R. Soc. Lond. A* (in the press); also as preprint astro-ph/9810196 (1998).
30. Zaldarriaga, M., Spergel, D. N. & Seljak, U. Microwave background constraints on cosmological parameters. *Astrophys. J.* **488**, 1–13 (1997).

A metal complex that binds α-amino acids with high and predictable stereospecificity

Jik Chin*, Soo Suk Lee*, Kyung Joo Lee†, Seongsoon Park* & Dong H. Kim†

* *Department of Chemistry, McGill University, 801 Sherbrooke St. W., Montreal, Canada H3A 2K6*
† *Center for Biofunctional Molecules, Pohang University of Science and Technology, Pohang 790-784, Korea*

Molecular recognition is the key step in a wide range of controlled separation and chemical transformation processes, with enzymes performing this task with an unsurpassed degree of selectivity. Enzymes contain only 20 simple amino acids, yet it remains difficult to rationalize or even predict these stereospecific recognition events. Nonetheless, the rational design of receptors able to recognize amino acids stereospecifically is attracting considerable interest because therapeutic drugs, that may be developed from chiral amino acid intermediates, are increasingly required in enantiomerically pure form[1]. Early work[2–4] has stimulated the development of efficient receptors based on small molecules[5–8], but binding of amino acids with high and predictable stereospecificity remains difficult to achieve. Directed molecular evolution[9], on the other hand, does select for RNA sequences or antibodies that bind amino acids with high specificity[10–12], but typically without providing insights into the molecular recognition mechanisms involved. Here we show that a rationally

designed metal complex formed from a trivalent cobalt ion and a tetradentate ligand binds natural amino acids, including the simple yet challenging amino acid alanine, with high and predictable regio- and stereospecificity. We expect that our approach will allow the binding as well as separation and stereospecific catalytic formation of its target amino acids.

There is much interest in rationally designing chiral metal complexes that bind or transform their targets, whatever they may be, with high and predictable stereospecificity. However, it has been a challenge to rationalize even the sense of the observed stereospecificity in simple binding or catalytic processes[13–15].

Octahedral metal complexes have often been used for stereospecific recognition of natural amino acids[16–19]. In order to control the regiospecific and stereospecific recognition of amino acids in a predictable way, we were interested in designing a chiral tetradentate ligand that forms only one isomer of an octahedral metal complex. Compound **1**, an unnatural α-amino acid, can form only one configurational isomer of an octahedral metal complex (**2**) due to the relative position of the four coordinating atoms (Fig. 1). Furthermore, molecular mechanics calculations show that **2** essentially exists as one conformational isomer. The [1,2,3] bicyclic portion of **2** (sharing the amino group bridge) is conformationally rigid, and the other five-membered ring in the complex (containing the dimethyl amine group) has only two possible conformations of which the one shown (**2**) is computed to be about a million times more populated than the other at equilibrium at 25 °C. Indeed, the crystal structure of the dinitro Co(III) complex formed from **1** is that of **2** (Fig. 2a).

In designing the tetradentate ligand (**1**) we reasoned that the carboxylate group of the ligand might prefer to coordinate *trans* to the carboxylate group of alanine (Fig. 1, **3a**) as has been shown for square planar bis-glycine complexes of Ni(II), Cu(II) and Zn(II) (ref. 20). Once regiospecific coordination of alanine is controlled, stereospecific coordination of alanine may be considered. Alanine forms a five-membered ring upon chelation to the metal complex (**3a**). In such five-membered rings the alanine methyl group is expected to occupy the equatorial position to avoid steric congestion with the coordinated atoms[21]. The α-H of the chelated alanine therefore has to occupy one of the two axial positions (Fig. 1, **3a** or **3b**). If one of these two axial positions is blocked with the dimethyl amine group of the tetradentate ligand, stereospecific recognition of alanine should result (that is, **3a** should be favoured over **3b**). Before synthesizing the tetradentate ligand, we carried out molecular mechanics calculations on **3a** and **3b**. In accordance with the

above reasoning, the computed energy value for **3a** is lower than that for **3b** by about 3 kcal mol^{-1}. It is also evident from computation that the α-H of alanine in **3b** comes in direct contact with one of the two methyl groups in the dimethyl amine group.

Compounds **1** and **2** were synthesized as racemic mixtures according to the path in Fig. 3. Addition of an equivalent amount of (±)-alanine to a racemic mixture of the dichloro cobalt complex (prepared from **2**) gave two main products **3a** and **3b** (each as a
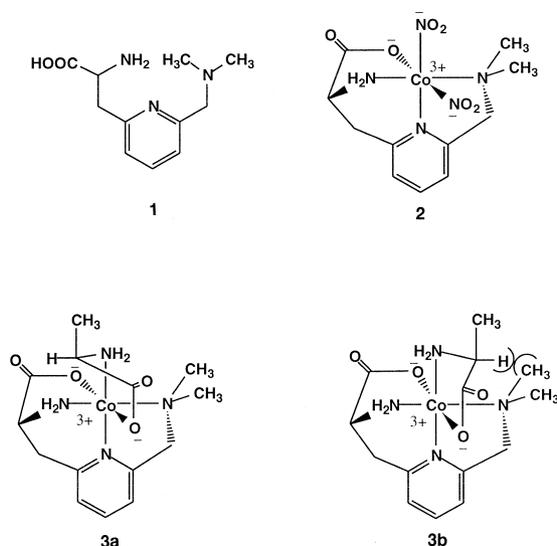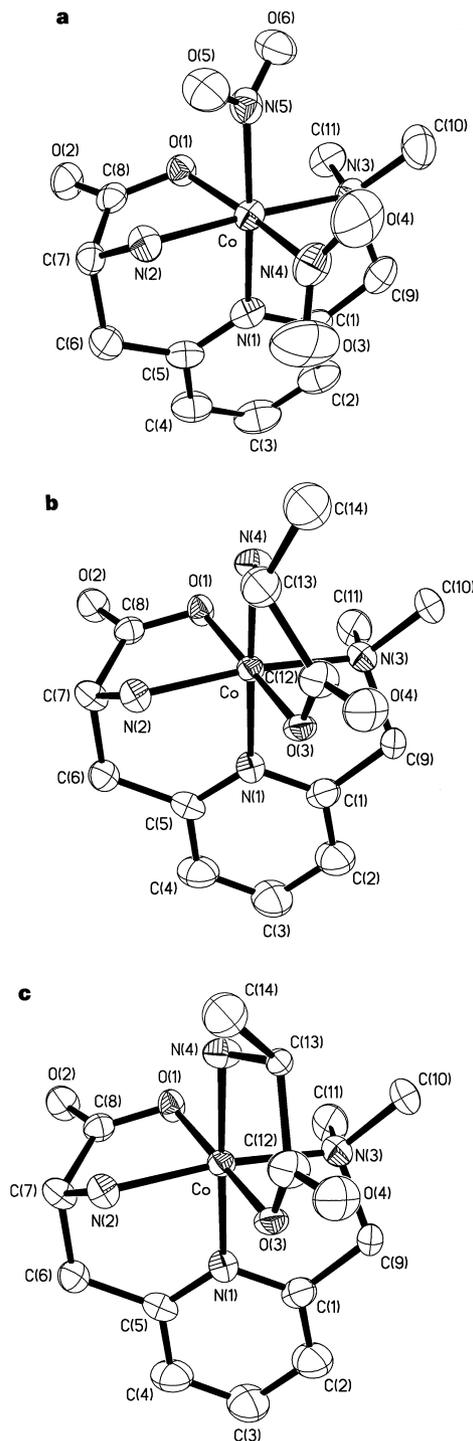
Figure 2 X-ray structures of cobalt complexes **2** (in panel **a**), **3a** (in panel **b**) and **3b** (in panel **c**): ORTEP representation with ellipsoids at the 20% probability level. Crystal structural data for purple square plates of a mixture of **3a**(ClO$_4$) and **3b**(ClO$_4$): orthorhombic, space group P2$_1$2$_1$2$_1$, $a = 9.620(3)$ Å, $b = 10.732(3)$ Å, $c = 19.710(4)$ Å, $Z = 4$; $R = 0.0461$, GOF = 0.787.

Figure 1 Structures of free chiral ligand (**1**), chiral cobalt complex (**2**) and alanine bound chiral cobalt complexes (**3a** and **3b**).
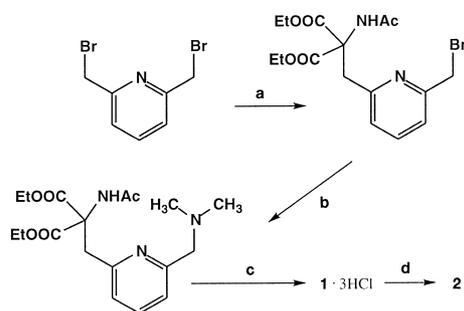
Figure 3 Reagents and conditions for the synthesis of **1** and **2**. **a**, Diethyl acetaminomalonate (1 eq.), NaH, TFH, 60 °C; **b**, Me$_2$NH in CH$_3$CN; **c**, 6 N HCl, reflux for 12 h; **d**, (i) 4 eq. NaOH (ii) [Co(III)(NO$_2$)$_6$]Na$_3$, 20 °C for 2 h.

racemic mixture). This mixture of **3a** and **3b** (Fig. 2b, c) was crystallized and subjected to crystallographic analysis revealing one racemic compound with temperature independent disorder for positions C13 and C14. We interpret this disorder to be caused by the presence of both diastereomers in the unit cell (data analysis gave ~70% **3a** and ~30% **3b** in the crystal mixture). The X-ray structures of **3a** and **3b** (Fig. 2b, c) are precisely in accord with the rational design. The two carboxylate oxygens (O1 and O3) in **3a** and **3b** are positioned *trans* to each other establishing regiospecific binding of alanine. The alanine methyl groups (C14) in **3a** and **3b** are in equatorial positions as predicted. The C13 hydrogen (α-H of alanine) of **3b** points towards the C10 carbon while that of **3a** points away from the C10 carbon. All of these features are in accord with the rational design.

Results of 500 MHz ^{1}H NMR scanning of the above crystalline mixture of **3a** and **3b** (again both racemic) indicate that the ratio of the two diastereomers in the crystal is about 60/40 (Fig. 4a); in reasonable agreement with the ratio obtained from the crystallographic analysis (70/30). Most of the signals for **3a** overlap with those for **3b** but two of the three methyl peaks (*a* and *c* peaks) are well enough separated to allow observation of the 60/40 diastereomeric ratio (see Fig. 4a). The *a* peak corresponds to one of the methyl groups of the tetradentate ligand and the *c* peak corresponds to the alanine methyl group.

Interestingly, **3b** epimerizes to **3a** in basic D$_2$O (Figs 4, 5). The *c*(**3a**) doublet rapidly disappears (Fig. 4a, b) to completion with a concomitant increase in the *c*(**3a-D**) singlet. This indicates that essentially all of **3a** has been deuterated. The *c*(**3b**) doublet also decreases but much more slowly than the *c*(**3a**) doublet. Conversion of **3b** to **I** (Fig. 5) is expected to be slower than conversion of **3a** to **I** (Fig. 5) since the α-H of alanine in **3b** is sterically more hindered. Similarly, deuteration of **I** is expected to take place more rapidly from the less hindered side to give more **3a-D** than **3b-D**. Consistent with this interpretation, we do not observe a signal for the *c*(**3b-D**) singlet (Fig. 4b). Although the signal due to a small amount of **3b-D** may be buried, integration of all the peaks in Fig. 4b (the integration ratio is 24:52:11:65 for peaks downfield to upfield with the two most upfield peaks integrated together) reveals that the amount of **3b-D** is unlikely to be more than 5% that of **3a-D**. It is clear from the above that the metal complex formed from the L-stereoisomer of **1** binds to the L-stereoisomer of alanine under thermodynamic control. The deuteration reaction shown in Fig. 5 implies that alkylation of **3a** and **3b** may also take place stereospecifically.

The fundamental concepts used here to develop the chiral metal complex for regiospecific and stereospecific recognition of alanine should be applicable for other bidentate α-H-amino acids. In order to investigate this possibility, we synthesized the receptor metal complex in enantiomerically pure form with a methyl group at the position of the α-hydrogen. This receptor in the *R*-form (which cannot be racemized due to the methyl group) was reacted with
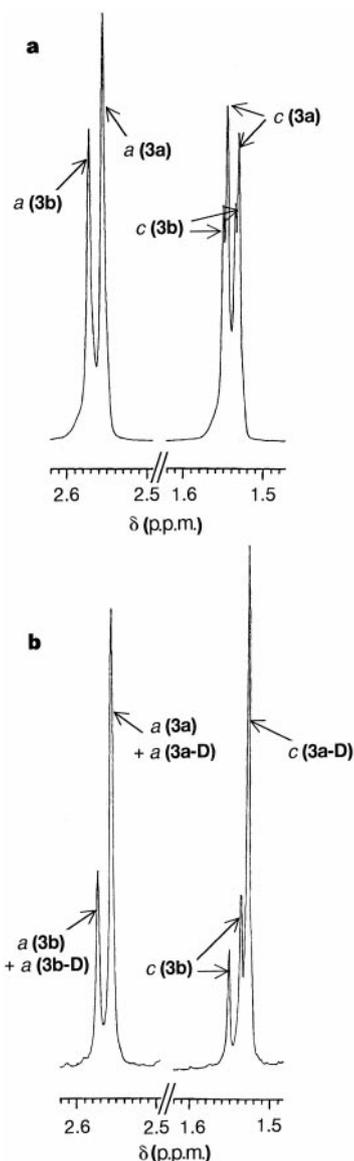

Figure 4 Characterization of the epimerization of **3a** and **3b**. Shown are 500 MHz ^{1}H NMR signals of one of the methyl groups of the tetradentate ligand (peak *a*) and the methyl group of alanine (peak *c*) in **3a** and **3b** (3 mM) before (panel **a**) and after (panel **b**) partial epimerization in 5 ml of 99.9% D$_2$O (5 mM NaOD, 50 h at 25 °C). In **a**, the integration ratios of *a*(**3a**)/*a*(**3b**) and *c*(**3a**)/*c*(**3b**) are both about 60/40. After partial epimerization (**b**), all of the *c*(**3a**) doublet has been converted to the *c*(**3a-D**) singlet. Also, peaks *a*(**3b**) and *c*(**3b**) have decreased but there is no evidence for *c*(**3b-D**).

glycine, L-alanine, D-alanine, L-phenylalanine, D-phenylalanine, L-tryptophan, and D-tryptophan. Essentially one complex formed in each of the seven reactions. The seven products were purified by ion exchange chromatography and treated with base in D$_2$O (see Supplementary Information). The α-hydrogens of the three D-amino acid products exchanged rapidly and completely with little or no observable epimerization. In contrast, the α-hydrogens of the three L-amino acid products exchanged slowly with concomitant epimerization. We were not able to fully deuterate the L-amino acid complexes due to competing decomposition reactions. Thus, the *R*-form of the receptor not only binds more tightly to the D-forms of the amino acids but also converts the L-forms to the D-forms. Note that amino acids with side chains that can interact strongly with the receptor (by coordination or H-bonding) may behave differently from the above mentioned amino acids. Nevertheless, this study clearly sets the framework for stereospecific recognition of amino
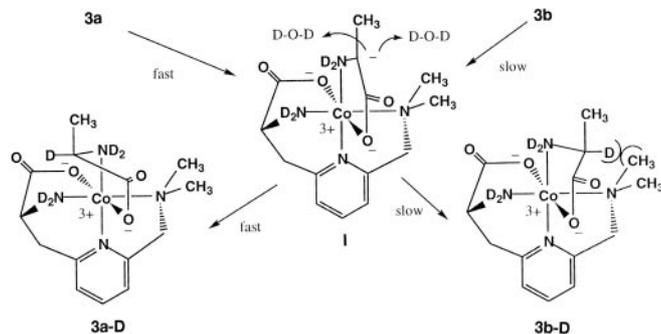
Figure 5 Mechanisms for deuteration/epimerization of **3a** and **3b** to **3a**-D and **3b**-D.

acids and, by implication, of structurally related molecules, such as chiral glycols, 1,2-diamines, 1,2-aminoalcohols, and α-hydroxy acids.

The X-ray crystallographic (Fig. 2) and ^{1}H NMR (Fig. 4) data show that coordination of alanine to our metal complex takes place with unprecedented regiospecificity and stereospecificity in accord with the design rationale. The regiospecificity is apparently controlled by electrostatic effects while the stereospecificity is controlled by steric effects in a highly predictive manner. This approach thus provides detailed structural insights into general separation of bidentate α-H-amino acids into D and L forms with a single chiral metal complex. Such a complex may also be useful as a catalyst for synthesizing α-H amino acids[22] or hydrolysing[23,24] their esters with predictable stereochemistry. □

1. Collins, A. N., Sheldrake, G. N. & Crosby, J. *Chirality in Industry* (Wiley and Sons, Chichester, Vol. 1, 1992 and Vol. 2, 1997).
2. Buckingham, D. A., Marzilli, L. G. & Sargeson, A. M. Proton exchange and mutarotation of chelated amino acids via carbanion intermediates. *J. Am. Chem. Soc.* **89**, 5133–5138 (1967).
3. Lehn, J.-M. & Sirlin, C. Molecular catalysis: Enhanced rates of thiolysis with high structural and chiral recognition in complexes of a reactive macrocyclic receptor molecule. *J. Chem. Soc. Chem. Commun.* 949–950 (1978).
4. Cram, D. J. The design of molecular hosts, guests, and their complexes. *Science* **240**, 760–767 (1988).
5. Zhang, X. X., Bradshaw, J. S. & Izatt, R. M. Enantiomeric recognition of amine compounds by chiral macrocyclic receptors. *Chem. Rev.* **97**, 3313–3361 (1997).
6. Kuroda, Y. *et al.* Chiral amino acid recognition by a porphyrin-based artificial receptor. *J. Am. Chem. Soc.* **117**, 10950–10958 (1995).
7. Still, W. C. Discovery of sequence-selective peptide binding by synthetic receptors using encoded combinatorial libraries. *Acc. Chem. Res.* **29**, 155–163 (1996).
8. Sessler, J. L., Andrievsky, A. Efficient transport of aromatic amino acids by sapphyrin-lasalocid conjugates. *Chem. Eur. J.* **4**, 159–167 (1998).
9. Joyce, G. F. Directed molecular evolution. *Sci. Am.* **12**, 92–97 (1992).
10. Famulok, M. & Szostak, J. W. Stereospecific recognition of tryptophan agarose by in vitro selected RNA. *J. Am. Chem. Soc.* **114**, 3990–3991 (1992).
11. Ellington, A. D. & Szostak, J. W. In vitro selection of RNA molecules that bind specific ligands. *Nature* **346**, 818–822 (1990).
12. Hofstetter, O., Hofstetter, H., Schurig, V., Wilchek, M. & Green, B. S. Antibodies can recognize the chiral center of free α-amino acids. *J. Am. Chem. Soc.* **120**, 3251–325 (1998).
13. Tokunaga, M., Larrow, J. F., Kakiuchi, F. & Jacobsen, E. N. Asymmetric catalysis with water: Efficient kinetic resolution of terminal epoxides by means of catalytic hydrolysis. *Science* **277**, 936–938 (1997).
14. Li, G., Chang, H.-T. & Sharpless, B. K. Catalytic asymmetric aminohydroxylation of olefins. *Angew. Chem. Int. Edn Engl.* **35**, 451–454 (1996).
15. Evans, D. A., Kozlowski, M. C., Burgey, C. S. & MacMillan, D. W. C. C₂ symmetric copper(II) complexes as chiral Lewis acids. Catalytic enantioselective aldol additions of enolsilanes to pyruvate esters. *J. Am. Chem. Soc.* **119**, 7893–7894 (1997).
16. Job, R. C. & Bruice, T. Chiral recognition of prochiral centers. *J. Am. Chem. Soc.* **96**, 809–819 (1974).
17. Yamaguchi, M. *et al.* Asymmetric transformation of α-amino acids promoted by optically active cobalt(III) complexes. *Inorg. Chem.* **19**, 2010–2016 (1980).
18. Fenton, R. R., Stephens, F. S., Vagg, R. S. & Williams, P. A. Chiral metal complexes 44. *Inorg. Chim. Acta* **236**, 109–115 (1995).
19. Fujii, Y., Matsufuru, M., Saito, A. & Tsuchiya, S. The stereochemistry and reactivity of metal-Schiff base complexes IV. *Bull. Chem. Soc. Jpn* **54**, 2029–2038 (1981).
20. Greenstein, J. P. & Winitz, M. *Chemistry of the Amino Acids* Vol. 1, 594 (Wiley and Sons, New York, 1996).
21. Zelewsky, A. *Stereochemistry of Coordination Compounds* (Wiley and Sons, Chichester, 1996).
22. Dabrowiak, J. C. & Cooke, D. W. Reaction of acetaldehyde with some optically active cobalt(III) complexes containing coordinated glycine. *Inorg. Chem.* **14**, 1305–1309 (1975).
23. Chin, J. Developing artificial hydrolytic metalloenzymes by a unified mechanistic approach. *Acc. Chem. Res.* **24**, 145–152 (1991).
24. Scrimin, P., Tecilla, P. & Tonellato, U. Chiral Lipophilic ligands: Enantioselective cleavage of α-amino acid esters in metallomicellar aggregates. *J. Org. Chem.* **59**, 4194–4201 (1994).

Cloud albedo enhancement by surface-active organic solutes in growing droplets

Maria Cristina Facchini*, **Mihaela Mircea***†, **Sandro Fuzzi*** & **Robert J. Charlson**‡

* *Istituto di Scienze dell'Atmosfera e dell'Oceano—Consiglio Nazionale delle Ricerche (ISAO-CNR), 40129 Bologna, Italy*
‡ *Departments of Atmospheric Sciences and Chemistry, University of Washington, Seattle, Washington 98195, USA*

Understanding the properties of clouds in the Earth's atmosphere is currently limited by difficulties at the fundamental level of adequately describing the processes of cloud droplet nucleation and growth. Small changes in droplet population may significantly influence cloud albedo[1] as well as formation of precipitation. Models of cloud formation based on laboratory studies with idealized composition of nuclei suggest that organic solutes significantly lower surface tension[2]—one of the parameters determining droplet population—but the lack of data on composition and properties of the organic material in the atmosphere precludes realistic laboratory or model studies. Here, we report measurements on vacuum-evaporated samples of cloud water from the Po Valley, Italy, that show a large decrease in surface tension, by up to about one-third relative to pure water, for realistic concentrations of organic solutes expected to exist in growing droplets. Such large surface-tension changes, if they occur in cloud droplets near the critical size for nucleation, lead to an increase in droplet population and hence in cloud albedo. The error produced in ignoring this effect is estimated to be comparable to other calculated direct and indirect influences of aerosols on scattering and absorption of solar radiation[3].

Traditional equilibrium (Köhler) theory[4] predicts that small (submicrometre) aerosol particles which are partially or completely water soluble act as cloud condensation nuclei (CCN) by lowering the vapour pressure and thus overcoming the requirement for large supersaturations caused by the small radius of curvature of the incipient droplets. The controlling variables would then be particle size and water-soluble mass; however, when measured, these alone do not accurately predict the CCN population[1]. Recently, additional variables have been proposed as factors that may also influence cloud droplet formation and properties. These variables include CCN solubility[2], droplet growth kinetics[5] and water-soluble gases[6]. Surface tension (σ), which is one of the factors that controls the vapour pressure of small droplets, is the consequence of intermolecular attractive forces tending to minimize the surface area of the liquid. Water has a high surface tension because of strong hydrogen bonds, the effect of which is diminished by the presence of surface-active solutes (surfactants).

Surface tension enters into the description of cloud droplet